

Adlakha, E., and Hattori, K., 2021, Thermotectonic events recorded by U-Pb geochronology and Zr-in-rutile thermometry of Ti oxides in basement rocks along the P2 fault, eastern Athabasca Basin, Saskatchewan, Canada: GSA Bulletin, <https://doi.org/10.1130/B35820.1>.

## Supplemental Material

### **SUPPLEMENTAL FILE 1**

**Figure A1.** Local geological map and cross-sections showing sample locations. (A) A plan view map showing the intersection of the P2 fault and associated faults at the unconformity of the Athabasca Basin. The major rock-types are shown in addition to the location of ore zones along the P2 fault. The location of the cross-sections in panels b to e are also shown (e.g., CS-B). The location of samples not shown in the following cross-sections are also indicated. Modified from Adlakha et al. (2020). (B–E) Schematic cross-sections of the P2 fault showing the sample locations in drill-core (stars). Cross-sections are simplified and were provided by Cameco. A small map showing the location of (A) and the Athabasca Basin, in addition to the Kivalliq Igneous Suite and the Thelon Basin, in Canada, is shown in the bottom left have corner.

**Figure A2.** Modelling results for the cooling age profiles of rutile in this study using the program DiffArg. The three piecewise linear models are for rutile with a radius of A) 250  $\mu\text{m}$ , B) 160  $\mu\text{m}$  and C) 50  $\mu\text{m}$ .

**Figure A3.** (A) A biplot showing the Concordia Age (Ma) vs Weighted Mean  $^{207}\text{Pb}/^{206}\text{Pb}$  age of rutile and anatase per sample. The ages and number of analyses are listed in Table 1. (B) A biplot showing the normalized spot location and  $^{207}\text{Pb}/^{206}\text{Pb}$  age for five rutile samples. Trendlines are shown for each population of rutile, and the low R-squared value is shown for the trendline of MAC99.

**Figure A4.** Box and Whisker plot showing the variation in calculated Zr-in-rutile temperatures per sample (listed in order below the graph). Circle markers represent individual analyses. The y-axis is scaled for 650 to 1000  $^{\circ}\text{C}$  to show the majority of the data and results of statistical calculations; however, there are a few outliers outside of this range. Outliers account for samples with a large difference between the mean (indicated by x) and median (see Supplemental File 2 for complete dataset including outliers).

**TABLE A1.** SAMPLE LIST AND DESCRIPTIONS, MODIFIED FROM ADLAKHA ET AL. (2020).

**TABLE A2.** RUNNING CONDITIONS OF THE LA-ICP-MS FOLLOWING HORSTWOOD ET AL. (2016).

### **SUPPLEMENTAL FILE 2**

Excel file containing U-Pb dataset for rutile and anatase, as well as Concordia diagrams and  $^{207}\text{Pb}/^{206}\text{Pb}$  weighted mean diagrams for each sample.

APPENDIX

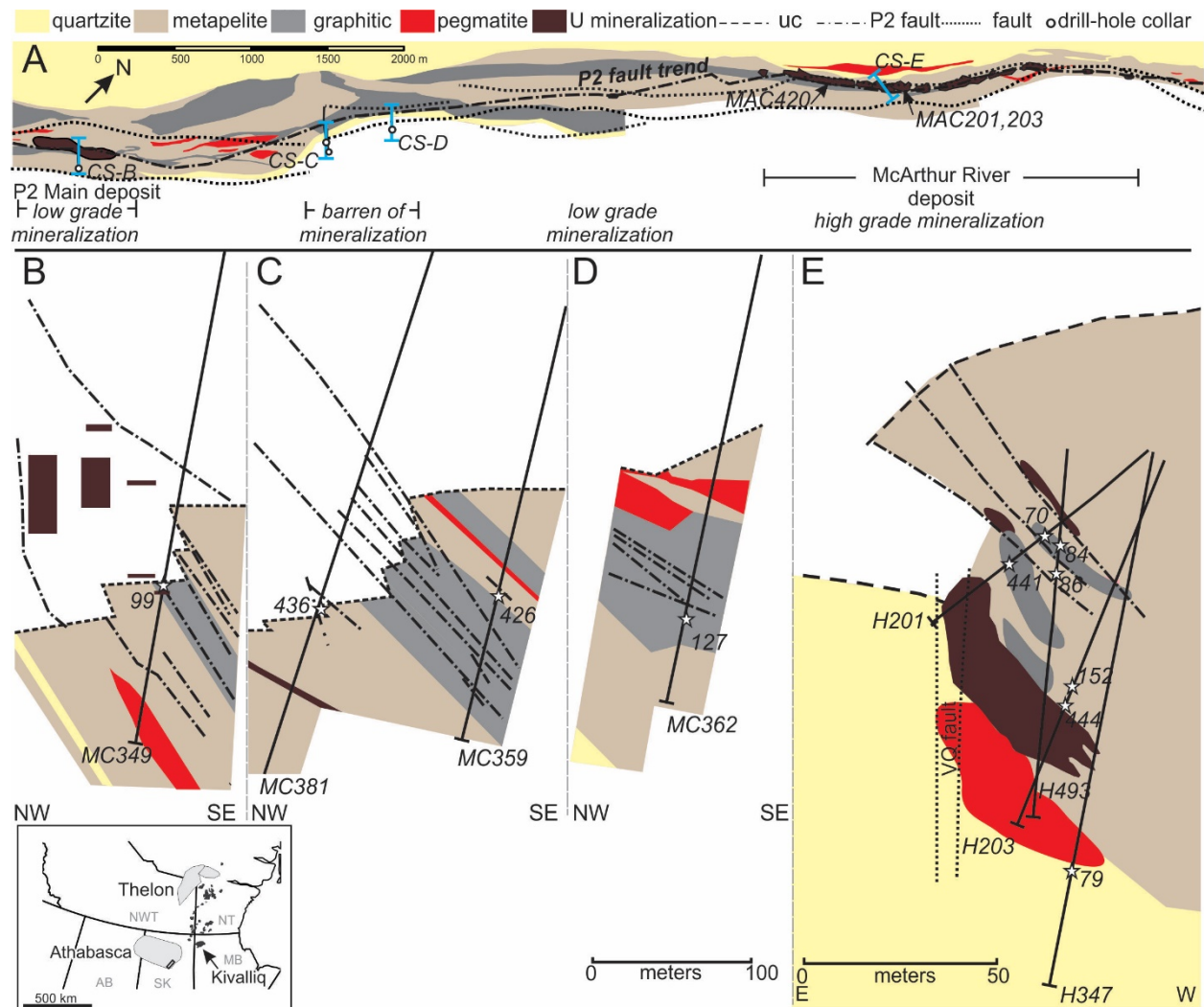


Figure A1: Local geological map and cross-sections showing sample locations. A) A plan view map showing the intersection of the P2 fault and associated faults at the unconformity of the Athabasca Basin. The major rock-types are shown in addition to the location of ore zones along the P2 fault. The location of the cross-sections in panels b to e are also shown (e.g., CS-B). The location of samples not shown in the following cross-sections are also indicated. Modified from Adlakha et al. (2020). B-E) Schematic cross-sections of the P2 fault showing the sample locations in drill-core (stars). Cross-sections are simplified and were provided by Cameco. A small map showing the location of (A) and the Athabasca Basin, in addition to the Kivalliq Igneous Suite and the Thelon Basin, in Canada, is shown in the bottom left have corner.

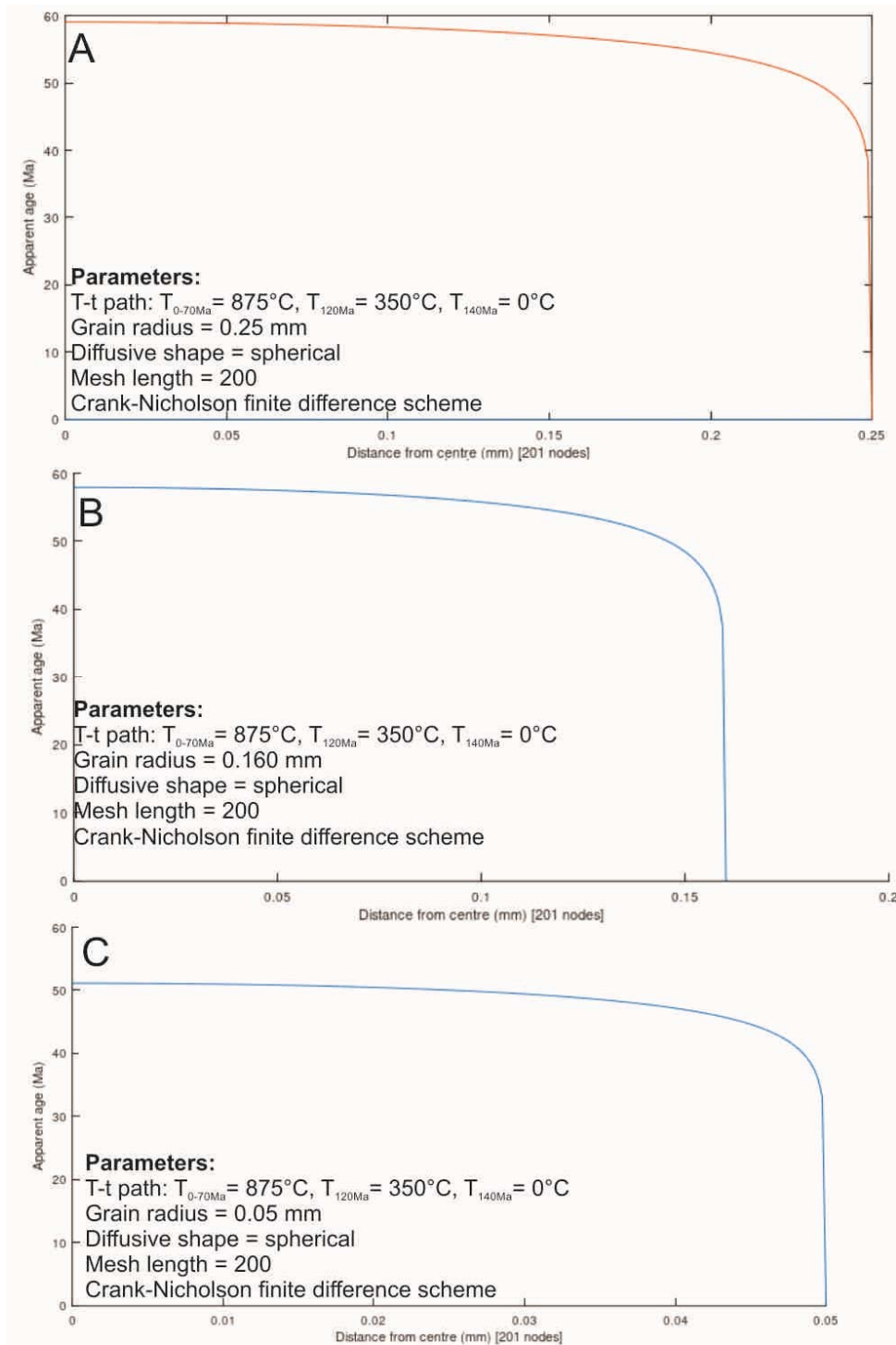


Figure A2: Modelling results for the cooling age profiles of rutile in this study using the program DiffArg. The three piecewise linear models are for rutile with a radius of A) 250  $\mu\text{m}$ , B) 160  $\mu\text{m}$  and C) 50  $\mu\text{m}$ .

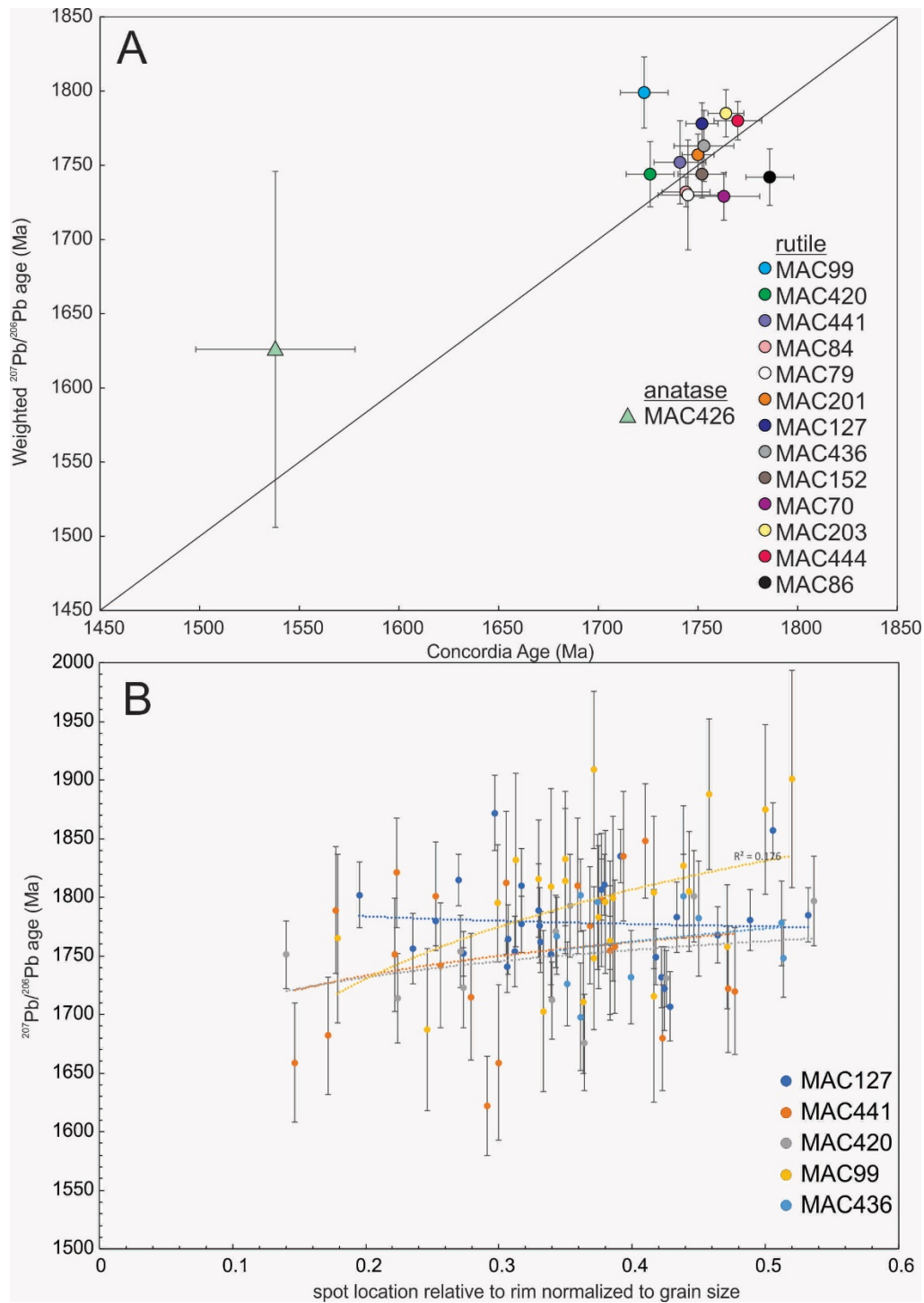


Figure A3: A) A biplot showing the Concordia Age (Ma) vs Weighted Mean  $^{207}\text{Pb}/^{206}\text{Pb}$  age of rutile and anatase per sample. The ages and number of analyses are listed in Table 1. B) A biplot showing the normalized spot location and  $^{207}\text{Pb}/^{206}\text{Pb}$  age for five rutile samples. Trendlines are shown for each population of rutile, and the low R-squared value is shown for the trendline of MAC99.

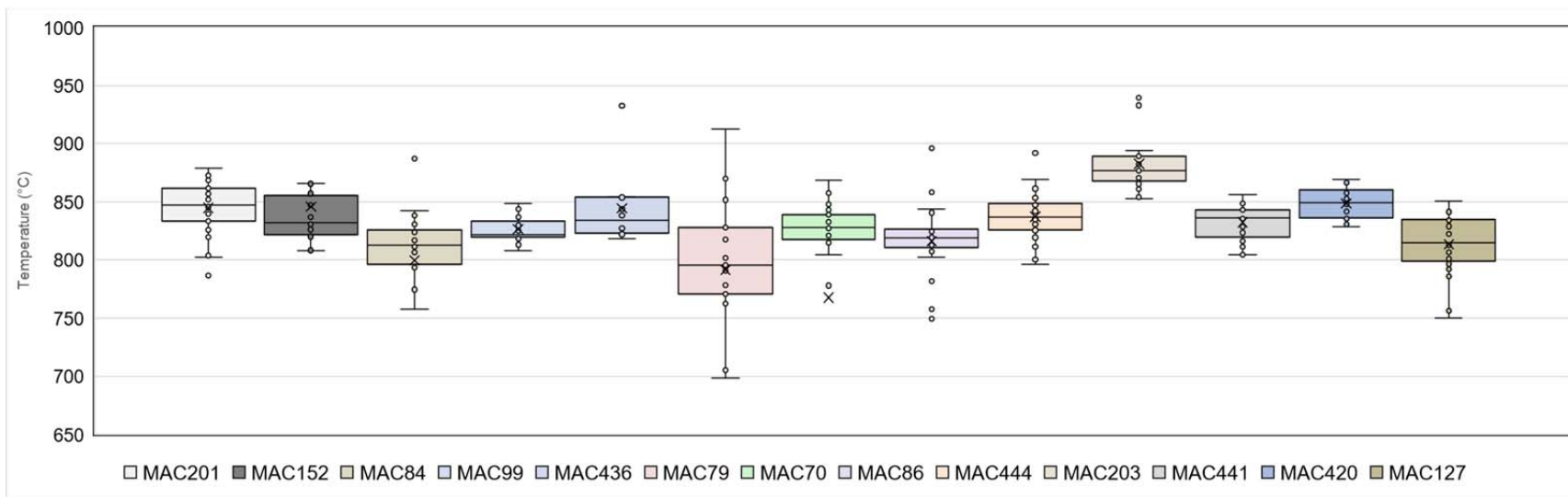


Figure A4: Box and Whisker plot showing the variation in calculated Zr-in-rutile temperatures per sample (listed in order below the graph). Circle markers represent individual analyses. The y-axis is scaled for 650 to 1000 °C to show the majority of the data and results of statistical calculations; however, there are a few outliers outside of this range. Outliers account for samples with a large difference between the mean (indicated by x) and median (see Supplemental File 2 for complete dataset including outliers).

TABLE A1: SAMPLE LIST AND DESCRIPTIONS, MODIFIED FROM ADLAKHA ET AL. (2020)

DDH <sup>a</sup>	Easting <sup>b</sup>	Northing <sup>b</sup>	Sample	Depth (m)	Lithology	Ti oxide mineral assemblage <sup>c</sup>	Ti oxide size (µm)	Ti oxide texture
MC349	493360	6397987	MAC99	573	quartz+oxy-dravite graphitic metapelite breccia with intense magnesio-foitite alteration	Rt-Qz-Dv-Ms-Zr	50 - 150	Subhedral, fractured crystals
H3559	496738	640096	MAC201	20.5	quartz+oxy-dravite vein in graphitic metapelite	Rt-Qz-Gr-Dv-Ms-Zr	50 - 500	Subhedral to rounded, clean to corroded rims
H3576	496912.3 0	6402209. 09	MAC203	55.7	metapelite with leucosome	Rt-Qz-Zr	200 - 400	Subhedral, heavily fractured with corroded rims
H203	496706.6 8	6402036. 94	MAC152	62	graphitic metapelite	Rt-Qz-Zr	100 - 400	Subhedral, fractured with corroded rims
H203	496706.6 8	6402036. 94	MAC444	69.7	graphitic metapelite with 1 cm wide leucosome	Rt-Qz-Gr-Ms-Zr	50 - 300	Subhedral, fractured with corroded rims
H201	496726	6402059	MAC70	34.3	graphitic metapelite breccia	Rt-Qz-Gr-Ms-Zr	20 - 100	Subhedral, fractured with corroded rims
H201	496726	6402059	MAC441	46.5	graphitic metapelite with leucosome patches	Rt-Qz-Gr-Ms-Zr	50 - 200	Subhedral, fractured with corroded rims
H347	496725.5 5	6402060. 37	MAC79	106	yellow-clay altered quartzite breccia	Rt-Qz-Sil-Ms-Zr	50 - 500	Sub-anhedral, fractured
H493	496715.8 4	6402080. 27	MAC84	24.5	quartz+oxy-dravite graphitic metapelite breccia	Rt-Qz-Gr-Dv-Zr-Py	50 - 200	Subhedral, fractured with corroded rims
H493	496715.8 4	6402080. 27	MAC86	31.7	graphitic metapelite breccia with leucosomes	Rt-Qz-Gr-Ms	50 - 150	Subhedral, fractured with corroded rims
H677	496483.0 3	6401838. 18	MAC420	57.1	metapelite with 10 cm wide pegmatite	Rt-Qz-Gr-Zr	50 - 400	Subhedral, fractured with corroded rims
MC362	494625.3 1	6399624. 84	MAC127	602.3	graphitic metapelite breccia with leucosomes	Rt-Qz- Gr-Dv-Zr-Py	40 - 250	Subhedral, fractured crystals
MC381	494386.1 3	6399253. 88	MAC436	603	quartz+oxy-dravite graphitic metapelite breccia with intense magnesio-foitite alteration	Rt-Qz-Dv-Zr	20 - 100	Euhedral, equant crystals with corroded rims
MC359	494441.9 1	6399221. 16	MAC426	581.6	local hematite-dolomite in graphitic metapelite	Ant-Dol-Hem	< 100	Euhedral to anhedral crystals with corroded rims

a: diamond drill hole.

b: UTM Zone 13, WGS-84, coordinates of DDH collar

c: Ant = anatase, Dol = dolomite, Dv = oxy-dravite, Gr = graphite. Hem = hematite, Ms = muscovite, P = pyrite, Qz = quartz, Rt = rutile, Sil = sillimanite, Zr = zircon

TABLE A2: RUNNING CONDITIONS OF THE LA-ICP-MS FOLLOWING HORSTWOOD ET AL. (2016)

Feature	Description
<u>Laboratory &amp; Sample Preparation</u>	
Laboratory name	Dept of Earth Science, University of New Brunswick
Sample type/mineral	Rutile and anatase
Sample preparation	100 um polished thick section, surface cleaned with methonal
Imaging	Petrographic microscope; BSE TESCAN MIRA 3 LMU Variable Pressure Schottky Field Emission SEM, 20 kV, 17mm working distance
<u>Laser ablation system</u>	
Make, Model & type	COMPexPro
Laser wavelength (nm)	193 nm
Fluence (J.cm <sup>-2</sup> )	2.9 J.cm <sup>-3</sup>
Repetition rate (Hz)	3 Hz
Ablation duration (secs)	30 secs
Ablation pit depth	7.2 um
Spot diameter (□m)	36 □m / 50 □m measured using an optical microscope
Sampling mode / pattern	Static spot ablation
Carrier gas	He in the cell, N <sub>2</sub> sampling-gas
Cell carrier gas flow (l/min)	He (300 ml/min), N <sub>2</sub> (2 ml/min)
<u>ICP-MS Instrument</u>	
Make, Model & type	Agilent 7700
Sample introduction	Ablation aerosol
RF power (W)	1550W
Masses measured & Integration time per peak/dwell times (s); quadrupole settling time between mass jumps	47Ti (0.01), 90Zr (0.01), 202Hg (0.04), 204Pb (0.06), 206Pb (0.04), 207Pb (0.06), 208Pb (0.01), 232Th (0.01), 238U (0.015)
<u>Data Processing</u>	
Gas blank	30 second on-peak zero subtracted
Calibration strategy	NIST610 used as primary reference material for concentrations and R10 as primary reference material for rutile geochron. R13 used as a QC standard
Reference Material info	NIST610 R10 (Luvizotto et al., 2009) R13 (Schmitt and Zack, 2012)
Data processing package used / Correction for LIEF	lolite add-on (Version 2.5). for Igor Pro (Version 6.3.7, Wavemetrics Inc.) for data normalization, uncertainty propagation and age calculation.
Quality control / Validation	R13 Concordia ages of 497.3 ± 7.3 (n = 10), 499.6 ± 6.9 (n = 10), and 498.2 ± 8.2 Ma (n = 8) for three sessions, within uncertainty of the published value (505±6 Ma; Schmidt and Zack 2012)